

AUG 18 2003

## REPORT DOCUMENTATION PAGE

AFRL-SR-AR-TR-03-

The public reporting burden for this collection of information is estimated to average 1 hour per response, including the gathering and maintaining the data needed, and completing and reviewing the collection of information. Send comments regarding this burden estimate or any other aspect of this collection of information, including suggestions for reducing the burden, to Department of Defense, Washington Headquarters Services, Directorate for Information Operations and Reports, 1215 Jefferson Davis Highway, Suite 1204, Arlington, VA 22202-4302. Respondents should be aware that notwithstanding any notice that may appear on this form that it is required by law to provide information, it is not subject to the collection of information if it does not display a currently valid OMB control number.

PLEASE DO NOT RETURN YOUR FORM TO THE ABOVE ADDRESS.

1. REPORT DATE (DD-MM-YYYY) 07/31/03		2. REPORT TYPE Final		3. DATES COVERED (From - To) 11/1/99-4/31/03	
4. TITLE AND SUBTITLE  Directional Recrystallization Processing				5a. CONTRACT NUMBER F49620-00-1-0076	
				5b. GRANT NUMBER	
				5c. PROGRAM ELEMENT NUMBER	
				5d. PROJECT NUMBER	
6. AUTHOR(S)  Ian Baker and H.J. Frost				5e. TASK NUMBER	
				5f. WORK UNIT NUMBER	
7. PERFORMING ORGANIZATION NAME(S) AND ADDRESS(ES)  Thayer School of Engineering, Dartmouth College Hanover, New Hampshire 03755				8. PERFORMING ORGANIZATION REPORT NUMBER	
9. SPONSORING/MONITORING AGENCY NAME(S) AND ADDRESS(ES)  Air Force Office Scientific Research 801N N. Randolph Street, Room 732 Arlington, VA 2203-1977				10. SPONSOR/MONITOR'S ACRONYM(S)  USAF/AFRF	
				11. SPONSOR/MONITOR'S REPORT NUMBER(S)	
12. DISTRIBUTION/AVAILABILITY STATEMENT  Approved for public release; distribution unlimited					
13. SUPPLEMENTARY NOTES					
14. ABSTRACT Fundamental research has been undertaken to understand how key microstructural parameters (grain size, particle spacing), interact with the processing conditions (temperature, rate of hot zone movement, temperature gradient in front of the hot zone) to control the microstructural evolution during directional recrystallization processing. The work involved close coupling of experiments with computer simulations. The computer simulation, in part, was to guide the choice of experimental parameters. A front-tracking grain-growth model was used to investigate the effects of hot zone width on the development of a columnar-grained structure and on its continued propagation. Analytical models were developed to explain both the critical hot zone velocity for the continued propagation of a columnar-grained structure and the relationship between the critical hot zone velocity and the hot zone width. The role of grain boundary energy and mobility on the development of a columnar grain structure were also explored. Experiments showed that most columnar grains produced in cold-rolled, directionally-recrystallized nickel have a {124}<21> orientation. Small island grains left inside the columnar grains were shown either to have low-angle boundaries or to be twins.					
15. SUBJECT TERMS  Direction recrystallization, single crystals, columnar grains, simulations					
16. SECURITY CLASSIFICATION OF:			17. LIMITATION OF ABSTRACT  UU	18. NUMBER OF PAGES	19a. NAME OF RESPONSIBLE PERSON Ian Baker
a. REPORT U	b. ABSTRACT U	c. THIS PAGE U			19b. TELEPHONE NUMBER (Include area code) (603) 646-2184

# DIRECTIONAL RECRYSTALLIZATION PROCESSING

I. Baker and H.J. Frost

Thayer School of Engineering, Dartmouth College, Hanover, NH 03755-8000.

## Research Objectives

The aim of this research was to understand how key microstructural parameters (grain size, particle spacing), interact with processing conditions (hot zone temperature, rate of hot zone movement, hot zone width, temperature gradient in front of the hot zone) to control the microstructural evolution during directional recrystallization. The work involved both experiments and computational simulation.

## Computer Simulation

A Front-tracking model developed by Frost et al.<sup>1</sup>, which simulates capillarity-driven grain growth in two-dimensions, was modified to simulate directional recrystallization. The algorithm follows each grain boundary segment as an array of moving points and alternates between moving all the boundary segments, and moving all the triple points, see Figure 1.

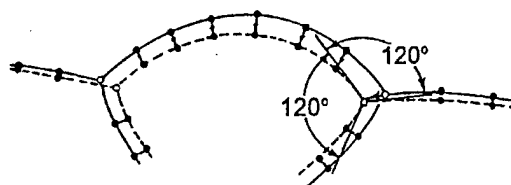


Figure 1: Schematic illustration of the front-tracking grain growth model.

Initially, only isotropic grain boundary energies and mobilities were considered, with the boundary velocity,  $v$ , given by  $v = \mu\kappa$ , where  $\mu$  is the mobility constant and  $\kappa$  is the local curvature. An infinite temperature gradient was used in all simulations, see Figure 2.

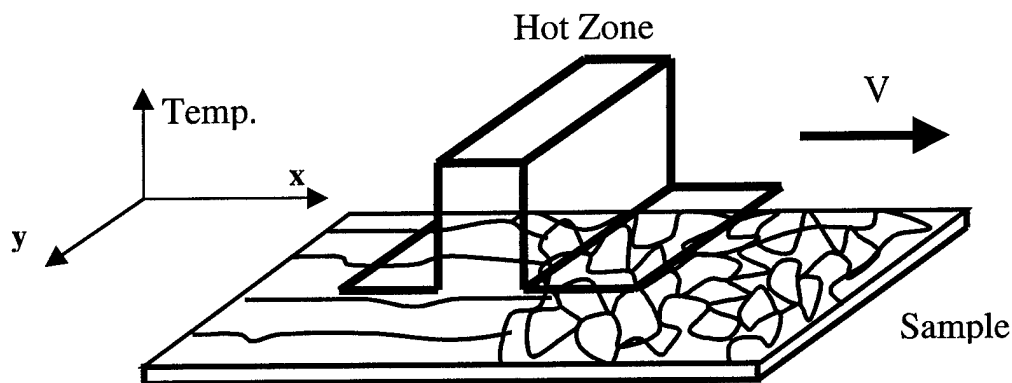


Figure 2: Moving hot zone with an infinite temperature gradient.

<sup>1</sup> H.J. Frost, C.W. Thompson and C.L. Howe and Junho Whang, "A Two-Dimensional Computer Simulation of Capillarity-Driven Grain Growth", *Scripta Metallurgica* 22 (1988) 65-70.

20030915 006

Later, anisotropy was included in the boundary energies and mobilities. In this case, the grain boundary migration velocity,  $v$ , was given by the product of not only the grain boundary mobility and the local curvature, but also the grain boundary energy. The variation in the mobility constant,  $\mu$ , can result either from variability in the mobility or from the variability in the boundary energy. In these simulations, for simplicity, a  $\langle 111 \rangle$  tilt boundary system was assumed, and the variability of the boundary energy and mobility only depended on the misorientation angle. Every grain was assigned an orientation angle randomly within the range  $1$ - $120^\circ$  at the beginning of the simulation. The misorientation angle between neighboring grains was calculated from the difference between their orientation angles. Grain boundary energy and mobility values were assigned according to Figure 3.

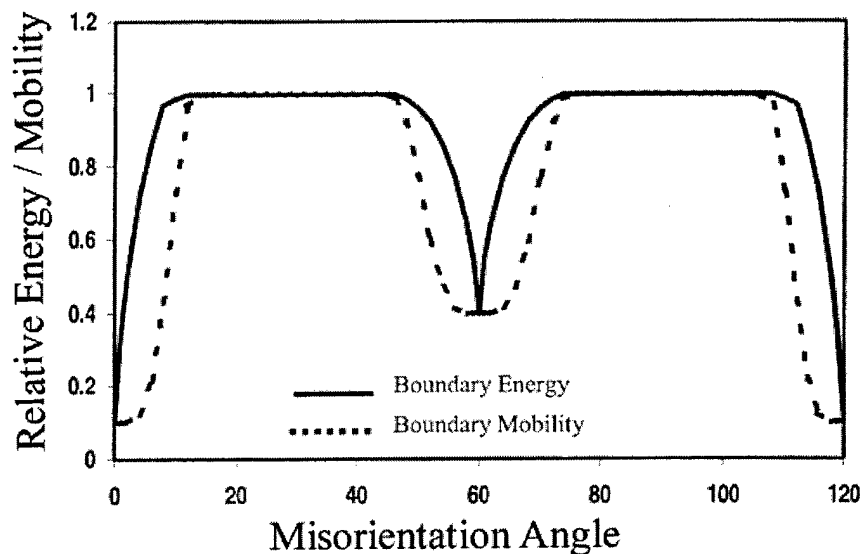


Figure 3. Relative grain boundary energy and mobility as a function of misorientation angle.

The simulation time was presented in a normalized dimensionless unit as  $\tau = t\mu/A_0$ , where,  $A_0$  was the initial average grain area and the mobility,  $\mu$ , had units of  $m^2/s$ . The hot zone width,  $L$ , is given in length units, where a length unit was defined as the square root of the initial average grain area. The hot zone velocity,  $V$ , was defined as the number of length units per normalized time unit. The initial arrays contained approximately 1,800 grains of unit average area on a field of  $60 \times 30$  length units. Normally, only a portion of the sample length, necessary for the effect being discussed, is displayed.

## Simulation Results

### Normal versus columnar grain growth

Figure 4 shows a comparison of the equi-axed structures resulting from normal grain growth and the columnar grain structures that can be obtained when a hot zone is moved along the sample length.

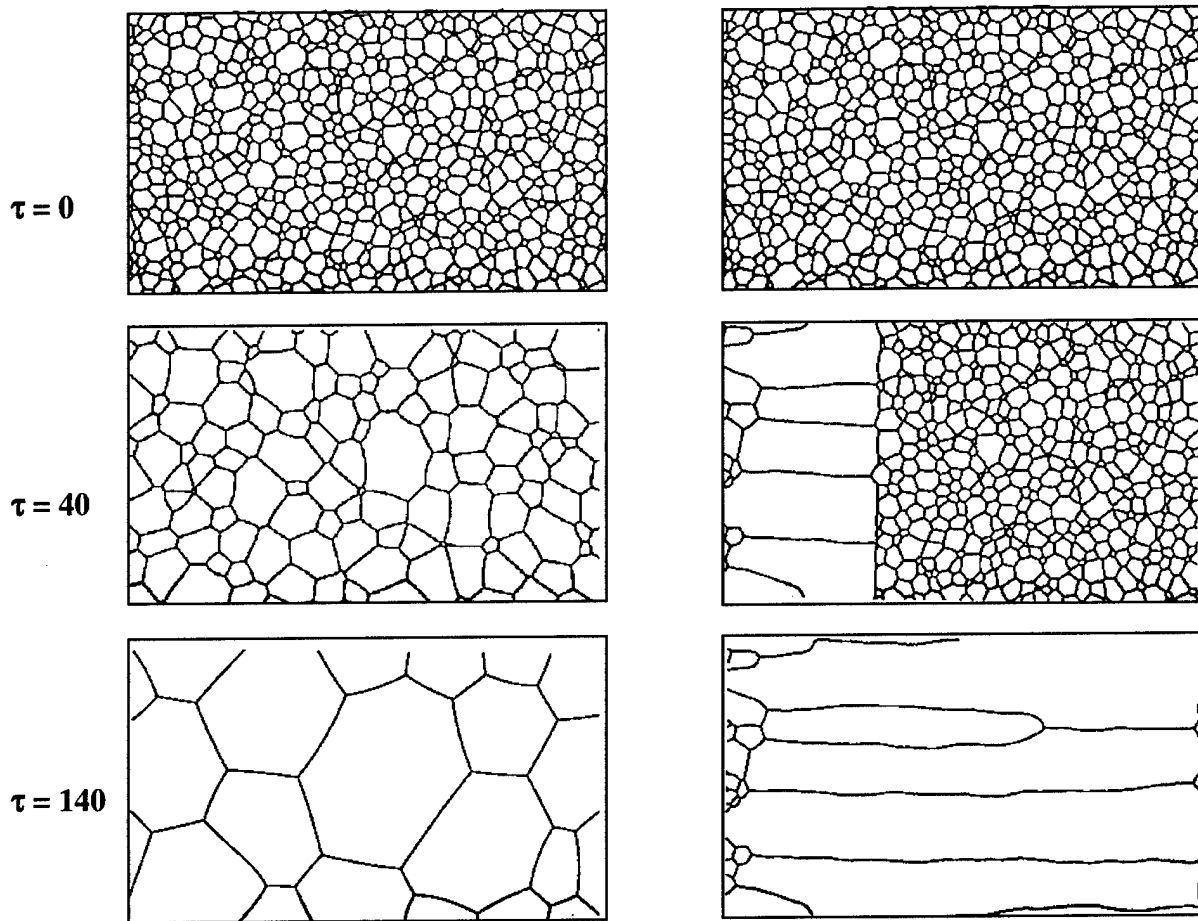


Figure 4: Normal grain growth versus grains resulting from a moving hot zone at three different times,  $\tau$ .  $L = 4$  and  $V = 0.25$ . Sample dimensions =  $30 \times 60$  length units.

## Effects of Hot Zone Velocity

Figure 5 shows structures formed with different hot zone velocities for two different initial structures. Columnar grains form and propagate only at lower velocities. Normal grain growth prevails when the hot zone speed is higher than the boundary mobility.

## Effect of Grain Boundary Mobility

Figure 6 shows that for a given hot zone speed, the structure depends on the grain boundary mobility. Higher mobility favors a columnar structure, since it enables grain boundaries to move more rapidly within the hot zone. Boundary migration is thermally activated. Thus, a higher mobility corresponds to a higher hot zone temperature.

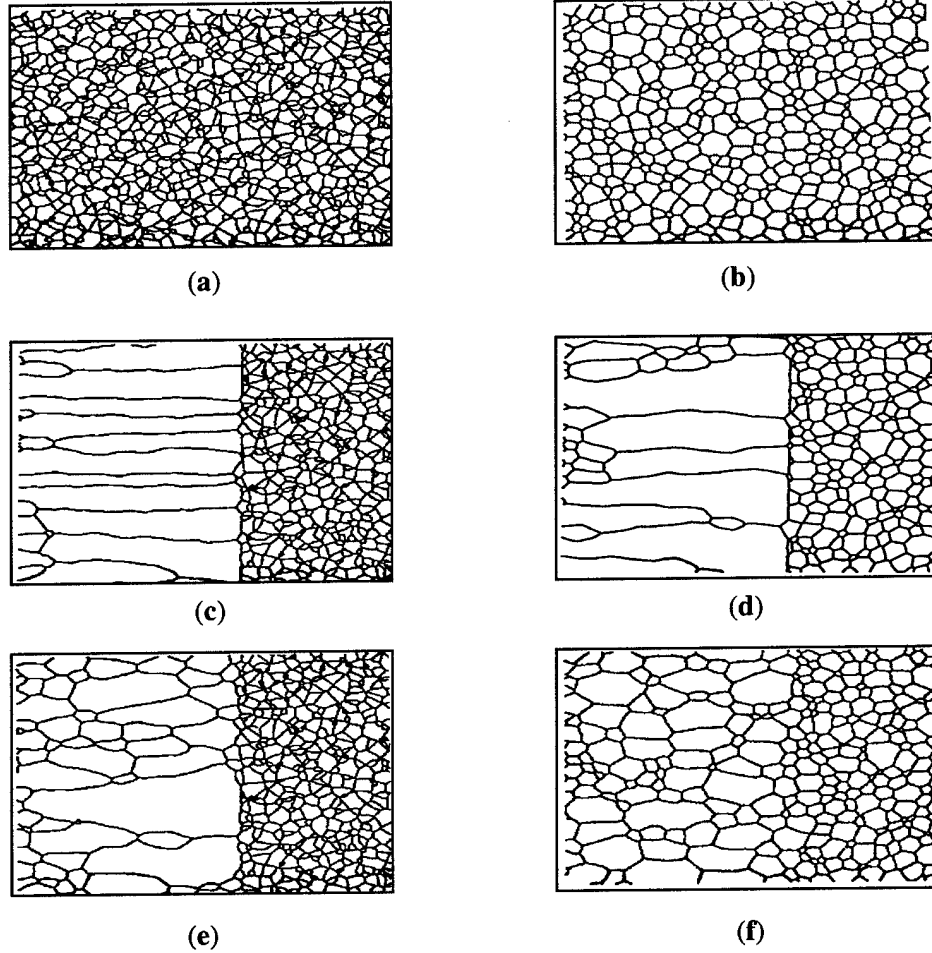


Figure 5. Effects of hot zone velocity for the two different initial structures shown in (a) and (b). (c),(d)  $V = 0.5$ ; (e),(f)  $V = 0.1$ . Sample dimensions =  $30 \times 40$  length units.

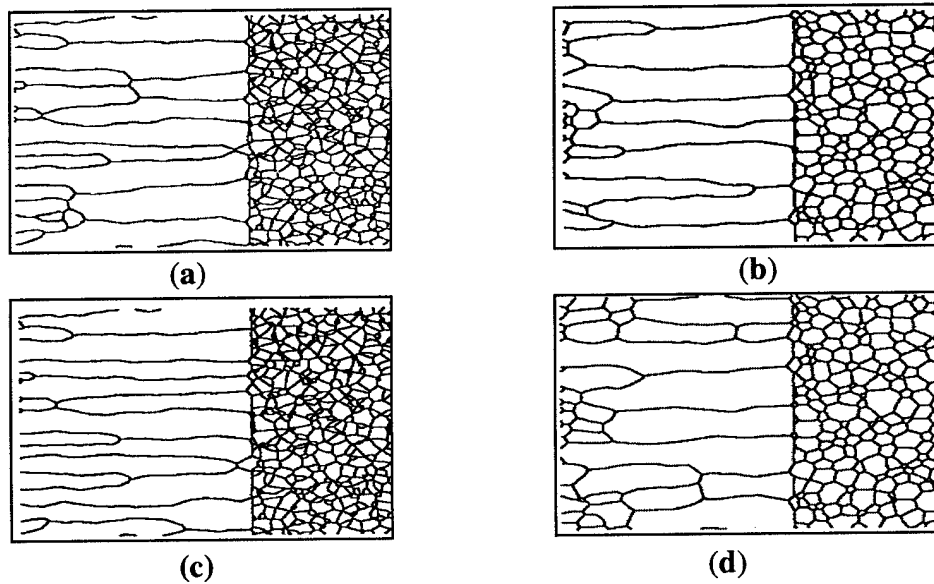


Figure 6. Effects of boundary mobility for different initial structures in Fig. 5. (a),(b) mobility = 0.005; (c),(d) mobility = 0.0005.  $V = 0.1$  and  $L = 2$ . Dimensions =  $30 \times 40$  length units.

*Effects of Hot Zone Width*

The effects of different hot zone widths on the development of a columnar grain structure are shown in Figure 7. For a given set of other parameters, the ease with which a columnar structure is formed increases with increasing hot zone width. The development of a fully columnar structure is shown to be virtually impossible for a hot zone width lower than about  $L = 1$  (Fig. 7a), i.e. about one initial grain diameter. A wider hot zone allows more time for grain growth and the formation of a growth front, which is aligned parallel with the hot zone and which is able to move with the hot zone. Moreover, the widths of the columnar grains increase with increasing hot zone width (Fig. 7b,c,d) because a greater time of residence in the wider hot zones allows greater lateral grain growth.

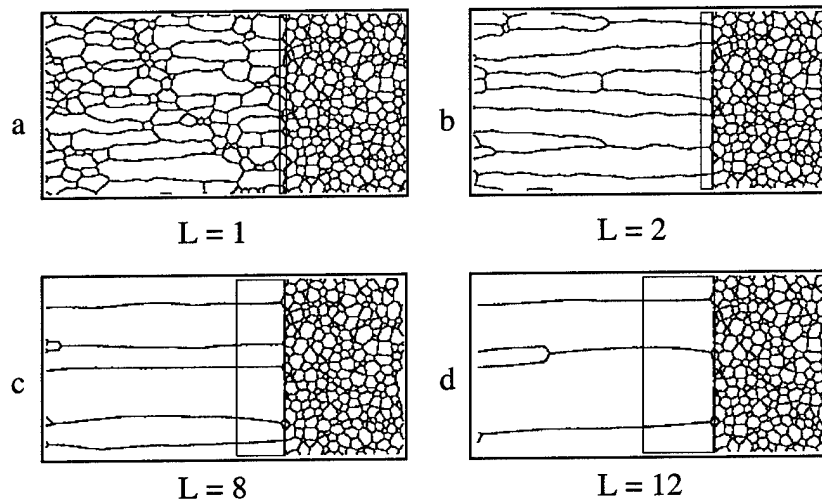


Figure 7. Effect of hot zone width on the development of columnar structure. Normalized hot zone velocity,  $V = 0.1$ . The positions and widths,  $L$ , of the hot zones are indicated.

The simulated structures were analyzed quantitatively and the results are shown in Figure 8 for the grain length and grain width as a function of hot zone velocity, for various hot zone widths. Because the entire lengths of the specimens were not processed and the lengths over which the hot zone was moved are different for the different samples, the measurements were taken over the processed regions with a uniform dimension of  $45 \times 30$  length units. The measurements were made using the linear intercept technique. The grain lengths are shown with solid lines and the corresponding grain widths are shown with broken lines. For a given hot zone width, the difference between the grain length and width decreases with increasing hot zone velocity. The grain length decreases considerably with increasing hot zone velocity whereas the grain width decreases only slightly. Generally, there are three characteristic hot zone velocity regions, high, intermediate and low. In the high velocity region, the grain structures are equiaxed and the effect of the hot zone width on the grain size is negligible. In the intermediate velocity region, grain length decreases rapidly with increasing hot zone velocity whereas the grain width decreases only slightly. In the low velocity region, there is no appreciable effect of velocity on the grain length and width. Although, in the limit, when the hot zone velocity is zero, no grain growth can occur.

The grain width increases with increasing hot zone width in all velocities, although only very slightly in the high velocity region. This is due to a longer time of residence in the wider hot zone. The average length of the elongated grains in the intermediate region, when the structure is not fully columnar, appears to increase with increasing hot zone width. Similarly, in the low velocity region, when the structure is fully columnar, the grain length increases with increasing hot zone width. However, in the latter case, since many of the grains transverse the entire length of the specimen for hot zone widths greater than  $L = 2$ , the grain lengths in Figure 8 represent only a lower limit on the grain length. Simulations of greater length would probably produce greater grain lengths.

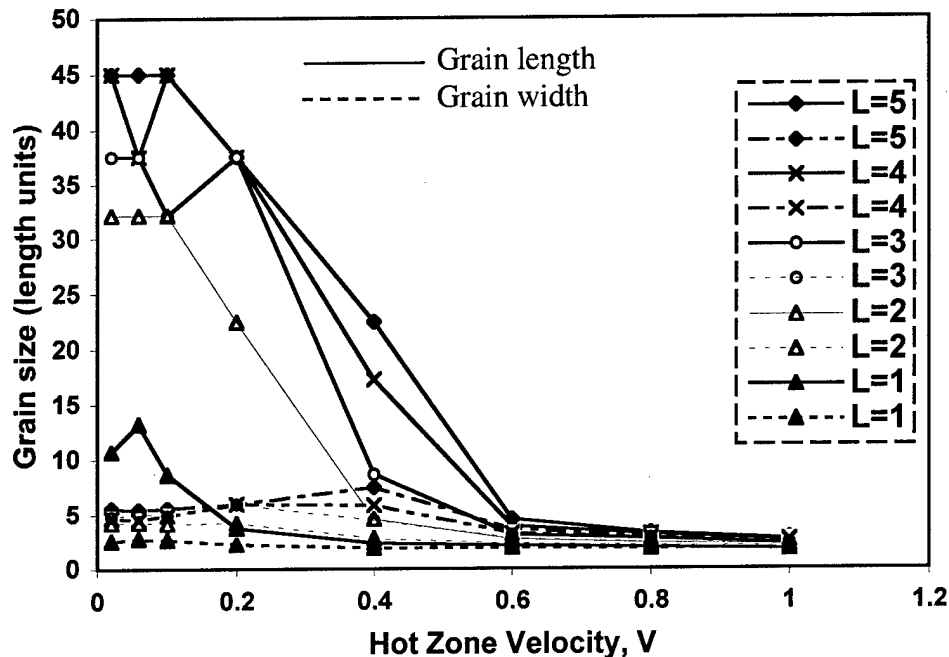


Figure 8. Grain length and width as a function of hot zone velocity and hot zone width.

#### Nucleation versus propagation of columnar grains

Figure 9 shows the effect of hot zone width on the *continued* propagation of a columnar grain structure. Starting the directional annealing process with a large hot zone width (Figure 9a) developed an initial columnar structure, with a aligned growth front. The hot zone width was then reduced and the directional annealing continued. It is evident that for a given hot zone velocity, the critical hot zone width for the propagation of a columnar structure is lower than for its development. While the development of a columnar structure is shown to be infeasible with a hot zone of 1 unit length (Figure 7a), its continued propagation is found to be successful with the same width and velocity (Figure 9b). However, increasing the velocity with the same width causes the columnar growth to break down and many equi-axed grains are left behind (Figure 9c). Increasing the width at this velocity again allows the columnar structure to propagate (Figure 9d). Generally, for a smaller hot zone width, the critical speed necessary for the continued propagation of a columnar grain structure is lower (Figure 9c,d).

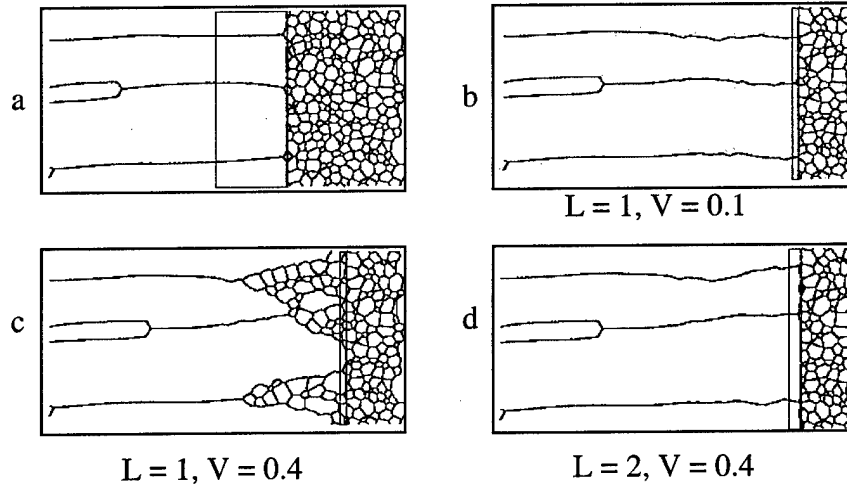


Figure 9. The effect of hot zone width on the continued propagation of columnar structure. The initial columnar grain structure in (a) was formed with  $L = 12$ ,  $V = 0.1$ . The positions and widths of the hot zones are indicated in each case.

## Critical velocity for propagation of columnar grains

Figure 10 shows the critical velocity for the *continued* propagation of a previously developed columnar structure as a function of hot zone width. For a given hot zone width, propagation of a columnar structure is feasible only for hot zone velocities at or below the critical velocity.

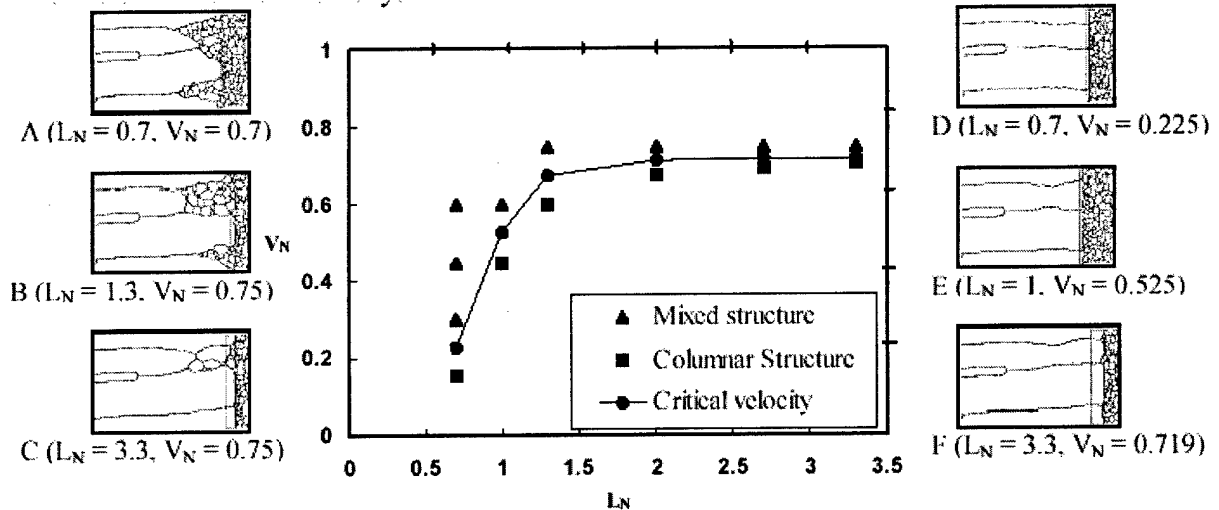


Figure 10. Graph of the normalized critical velocity,  $V_N$ , for the continued propagation of columnar structure as a function of the normalized hot zone width,  $L_N$ .

A simple analysis is outlined below using the schematic illustrations in Figure 11.



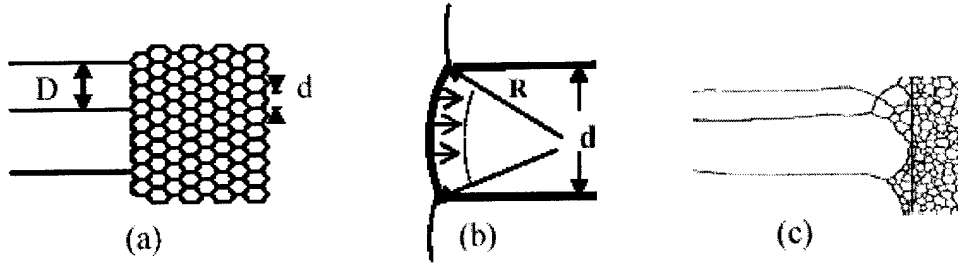


Figure 11. Schematic of the propagation of columnar grains. (a) columnar grains growing into an equi-axed grain structure ahead of the hot zone; (b) movement of an equi-axed grain boundary at the growth front in the hot zone, (c) retarding effect at the triple junctions linking the columnar grains with the equi-axed structure.

The grain boundary velocity is:

$$v = \mu k = \mu/R \quad (1)$$

where  $k$  is the local curvature and  $R$  is the radius of curvature of the boundary segment, (Figure 11b). Assuming that the equi-axed grain shape is hexagonal,  $R \approx d$  and  $v = \mu/d$ . Therefore, the critical hot zone velocity,  $V_N$ , in dimensionless form, above which the propagation of the columnar structure fails is:

$$V_N^* = (v A_0^{1/2}) / \mu = (\mu/d) \times (A_0^{1/2}) / \mu = A_0^{1/2}/d \approx 1 \quad (2)$$

However, the width of the columnar grain may have some retarding effect on the motion of the growth front. As illustrated in Figure 11 (c), the curvatures of the boundary segments at the connecting triple junctions between the columnar boundaries and the equi-axed grains are shallower than those of the other equi-axed grains at the growth front. The resulting slower movement at the connecting triple points retards the propagation of the columnar grain. This retarding effect is proposed to be equal to the ratio of the initial equi-axed grain size to the minimum columnar grain width,  $d/D$ . The critical velocity of the hot zone is then given as:

$$V_N = 1 - d/D \quad (3)$$

Calculations of the critical hot zone velocity were performed for the results shown in Figure 10, with initial equi-axed grain size,  $d = 1.5$  length units. Using structure C in Figure 10, the width,  $D$ , of the thinnest columnar grain at the point of breakdown is 5.3 length units. Putting these values into equation (3),  $V_N = 0.72$ . This result agrees well with the critical hot zone velocity of 0.72, obtained at the higher hot zone width region when the critical hot zone velocity is independent of the hot zone width (F in Figure 10).

The increase in critical velocity with increasing hot zone width in the low width region in Figure 10 is due to the structure of the growth front, which is characterized by ridges and valleys rather than a perfectly aligned smooth surface (Fig. 11c). Because of the slower movement of the triple points, the growth front appears to be pinned by the triple points in a similar way to that of a grain boundary bowing between particle dispersions. The various possible scenarios are illustrated in Figure 12.

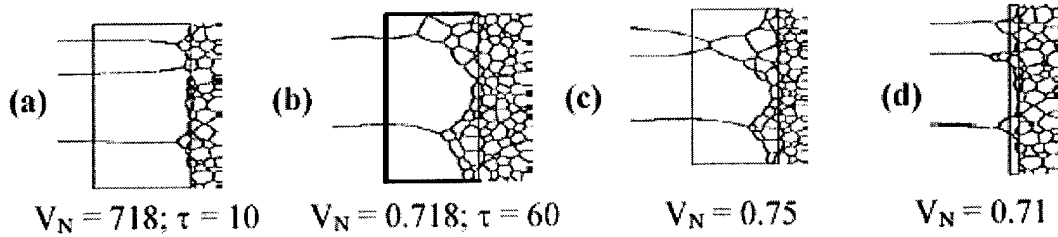


Figure 12. Illustrations of the effect of hot zone velocity and hot zone width on the evolution of the growth front in the propagation of a columnar-grained structure.

For a zone velocity higher than the velocity of the triple points, the growth front breaks down with ridges forming at the trailing triple points. At the critical velocity, the structure of the front evolves with time and two stages of evolution are distinguishable. In the initial stage, the size of the ridge is smaller than the average initial grain size and the growth front ahead of the trailing triple points aligns well with the leading end of the hot zone (Fig. 12a). In the final stage, the maximum ridge size exceeds the initial grain size and the growth front forms a concave shape with only a portion of it in contact with the leading end of the hot zone (Fig. 12 b). For a velocity below critical, evolution of the front is suppressed and the size of the ridges increases with increasing zone velocity. For a zone velocity lower than the velocity of the linking triple points, aligned growth front is propagated. Propagation is possible if the zone velocity is not higher than the critical velocity and the hot zone is large enough to contain the triple point ridges with, at least, a portion of the growth front in contact with the leading end of the hot zone (Fig. 12a,b). Propagation fails if the zone velocity is higher than the critical velocity, regardless of the hot zone width, because the growth front trails the leading end of the hot zone and grain growth occurs ahead of the growth front (Fig. 12c). If the hot zone width is too small, the triple point ridge grows beyond the hot zone and only the front portion of the growth front is contained in the hot zone, hence the propagation fails (Fig. 12d). Hence, in the low width region, the critical velocity is the velocity required to keep the trailing triple points within the hot zone and it increases with zone width (Fig.10). When the zone width is increased within the region of the initial stage, the critical velocity increases linearly because the whole of the growth front is aligned with the hot zone end and the advancement in the growth front is totally due to the increase in the hot zone width. The increase in the critical velocity due to the increasing hot zone width decreases as the portion of the growth front in contact with the leading end of the hot zone decreases. It eventually becomes zero when the growth front touches the hot zone only at a spot (Fig. 12b). This explains the decreasing gradient leading to the constant critical velocity in Figure 10. The critical velocity model is verified in Figure 13, which shows the effect of columnar grain widths on the propagation of a columnar grain structure. Propagation was not possible at a hot zone velocity of 0.6 for the sample with an initial average grain width of 4.3 length units (Fig. 13a), but possible for the sample with an average initial width of 10 length units (Fig. 13b). The thinner grain A in Figure 13 broke down whereas the larger grains B and C propagated at a higher zone velocity of 0.75. Consistent with the model, bigger initial columnar grain width favors propagation.

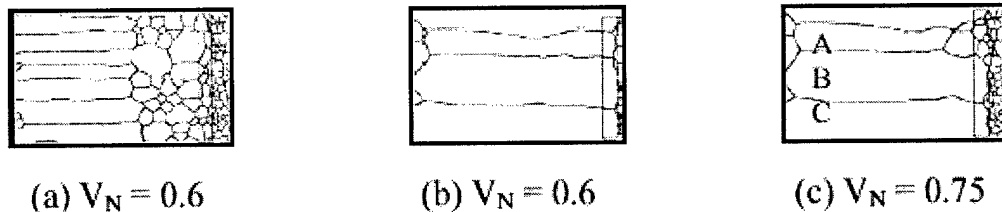


Figure 13. The effect of the columnar grain width on the critical velocity for the continued propagation of a columnar grain structure.

*Effect of anisotropic boundary properties on microstructural evolution*

Figure 14 shows the effect of variable boundary energy and mobility on the development of a columnar grain structure during directional annealing at different hot zone velocities. The development of a columnar grain structure is shown to be more difficult with a non-uniform grain boundary energy and mobility. With a constant boundary energy and mobility, a columnar grain structure is well formed at a very low hot zone velocity of 0.15 (Figure 14 (a)), fairly formed at a moderate velocity of 0.45 (Figure 14 (b)), and a mixed elongated and equi-axed grain structure is formed at a high velocity of 0.6 (Figure 14 (c)). With a variable energy and mobility, a somewhat elongated structure is formed at the lowest velocity (Figure 14 (d)), but with many low angle, small grains left inside. The structures formed at velocities of 0.45 and 0.6 are equi-axed structures interspersed with only a few slightly elongated grains (Figure 14 (e,f)). The boundary energy and mobility in the isotropic system are constant and at the maximum values. Therefore, the driving force for grain growth is at the highest level, making the development and propagation of a columnar grain structure easier. In the anisotropic system, the proportion of low angle/twin boundaries, with low energies and low mobilities is substantial, resulting in driving force variability along the growth front. Under this condition, the establishment of a smooth growth front for columnar grain propagation becomes difficult and where it occurs, keeping pace with the moving hot zone is difficult, and the low angle, and thus low energy, grains tend to be left behind the growth front. As shown in Figure 14, the same or similar colored grains clustered together, and thus formed low-angle grain boundaries between them.

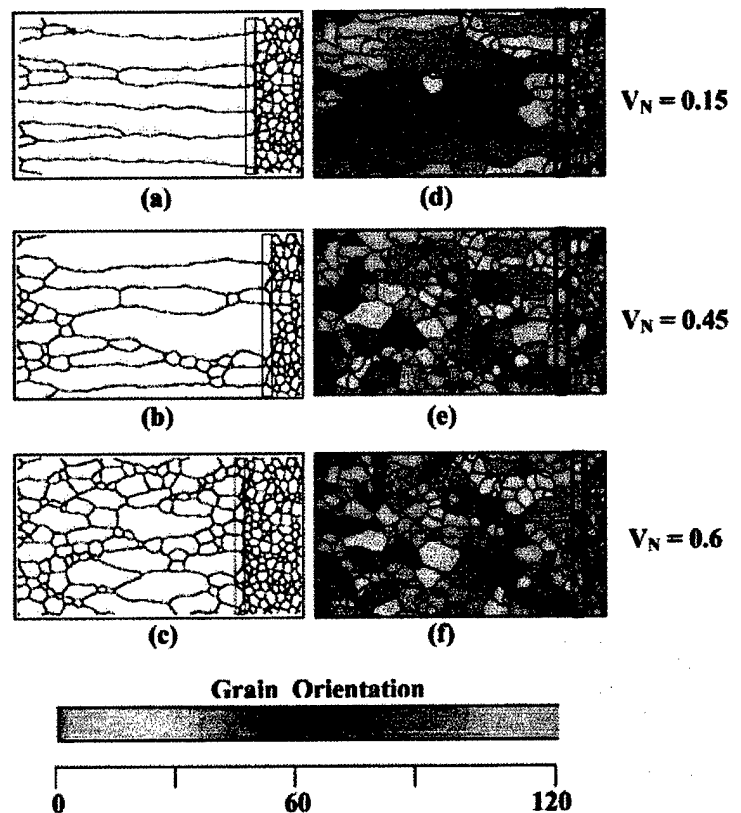


Figure 14. Effects of variable grain boundary energy and mobility on the development of columnar grain structure. Structures with variable boundary energy and mobility are shown in colors. The position and width of the hot zone are indicated.  $L_N = 1.3$ .

*Effect of hot zone width*

Figure 15 compares the effects of hot zone width on the development of columnar grain structures for the isotropic and anisotropic systems. In the isotropic system, the development of a columnar grain structure is shown to be enhanced with the width of columnar grains increasing with increasing hot zone width. In contrast, the effect of hot zone width appears to be negligible

on the development of columnar grain structure in the anisotropic system. The development of columnar grain structures comprises of the growth of the favorably oriented grains and the alignment of the growth front with the leading end of the hot zone. An increase in the width of the hot zone increases the residence time of the hot zone at a given location and the amount of growth that takes place, if the driving force for migration is sufficient. In an isotropic system, where the driving force is at a maximum, development of a columnar grain structure improves with increasing hot zone width. On the other hand, the low-angle boundaries in an anisotropic system are not mobile, making the development of columnar grain structure difficult and almost insensitive to changes in hot zone width.

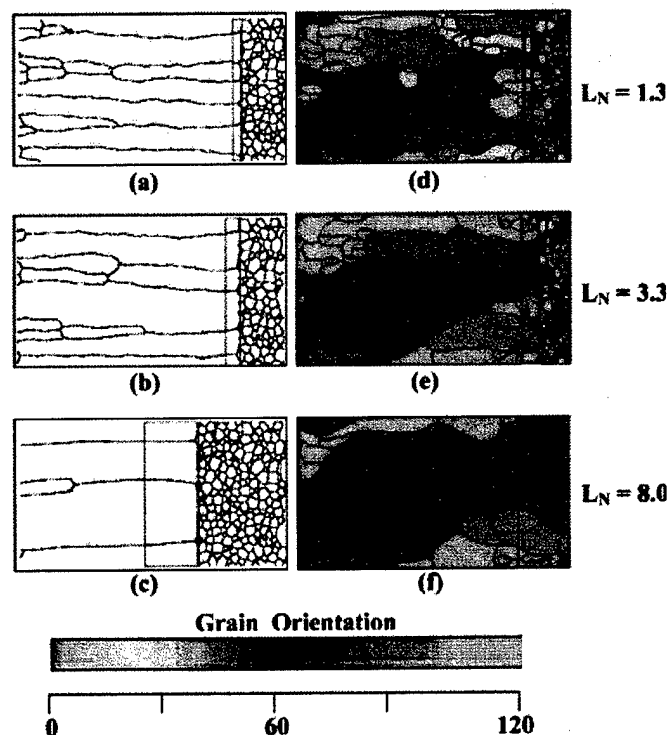


Figure 15 Effects of hot zone width on the development of columnar grain structure for variable and constant boundary energy and mobility. Structures with variable energy and mobility are shown in colors.  $V_N = 0.15$ .

## Directional Recrystallization of Nickel

The effects of annealing temperature, hot zone velocity and temperature gradient ahead of the hot zone on the directionally recrystallized microstructure were studied for both 90% cold-rolled and primary recrystallized (15  $\mu\text{m}$  grain size) polycrystalline nickel using a modified optical-image furnace.

### Effect of Hot zone velocity

It was found that columnar grain structures could only be produced by directional recrystallization over a limited range of hot zone velocities. In this range, limited nucleation and grain growth occurs and the grain boundaries have high enough mobility to keep up with the moving hot zone. At 1000°C and a temperature gradient of 1000°C/cm, bicrystals, 5 mm wide and > 14cm long, could be grown at hot zone velocities from 5 to 10 mm/h for cold-rolled nickel, and from 5 to 30 mm/h for primary recrystallized nickel. Equi-axed grains were produced when the hot zone velocity was outside these ranges.

### Effect of Hot zone temperature

Decreasing the hot zone temperature decreases the grain boundary mobility and shifts the optimum hot zone velocity range over which the columnar grain structure occurred to lower

velocity. However, at 370°C and 420°C, equi-axed grain structures, with an average grain size of 20  $\mu\text{m}$ , were produced at all hot zone velocities.

### *Effect of Temperature gradient ahead of the hot zone*

The temperature gradient ahead of the hot zone is a key parameter for directional recrystallization. Increasing temperature gradient decreases the specimen temperature ahead of the hot zone and, thus, prevents significant grain growth ahead of the hot zone. At 1000°C, reducing the temperature gradient to 50°C/cm produced equi-axed grains at hot zone velocities from 2 to 100 mm/h, the grain size decreasing with increasing hot zone velocity. In order to examine the effects of different temperature gradients further, runs were performed at 1000°C with a hot zone velocity of 100mm/h and temperature gradients of 1000°C/cm and 50°C/cm and terminated part way through. The microstructures ahead of the hot zone are shown in Figure 16. For the 1000°C/cm temperature gradient, there is a clear line between the large columnar grains and the growth front, Figure 16(a). Nucleation and grain growth do occur ahead of the hot zone as seen in Figure 16(b), but the average grain size is only 20  $\mu\text{m}$ . The columnar grains inside the hot zone have a size advantage over these small equiaxed grains, thus a columnar growth front was formed and a columnar grain structure was produced. Interestingly, the straight grain boundaries between grains were found to be twin boundaries. For the 50°C/cm temperature gradient, there is no clear line delineating the hot zone and the region ahead of it, seen Figure 16(c). Grains nucleated ahead of the hot zone grew to a significant grain size (0.8 mm in Figure 16(c)). The grains inside the hot zone lose their size advantage over the big grains ahead of the hot zone, thus an equi-axed grain structures was produced.

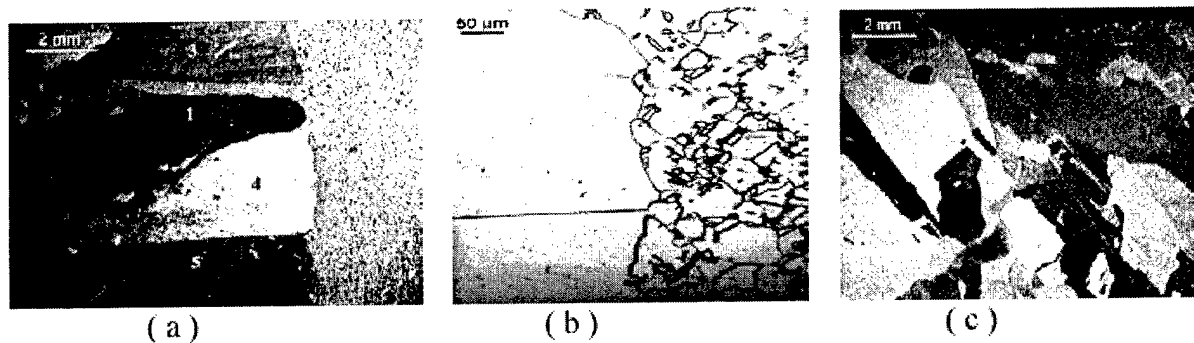


Figure 16. Microstructures ahead of a hot zone with a temperature gradient of (a, b) 1000°C/cm and (c) 50°C/cm.

### *Single Crystal growth*

Single crystals have been grown by directional recrystallization at 1000°C and 1000°C/cm temperature gradient, and a hot zone velocity of 5mm/h after prior primary recrystallized at 350°C, i.e. by directional *secondary* recrystallization. In contrast, we have not been able to grow single crystals of as-rolled nickel by directional recrystallization, even though the nickel undergoes primary recrystallization ahead of the hot zone to a microstructure similar to that of the nickel statically recrystallized at 350°C.

## Texture evolution in directional recrystallization of unalloyed nickel

The orientations of the columnar grains produced by directional recrystallization with a 1000°C hot zone temperature and a temperature gradient of 1000°C/cm of both 90% cold-rolled and 90% cold-rolled and primary recrystallized (20 µm grain size) polycrystalline nickel, were measured using a HKL EBSP system in a SEM, operated at 30 keV. The microstructures are shown in Figure 17. It is clearly seen that the columnar grains have a  $\{124\}\langle 21\bar{1}\rangle$  preferred orientation.

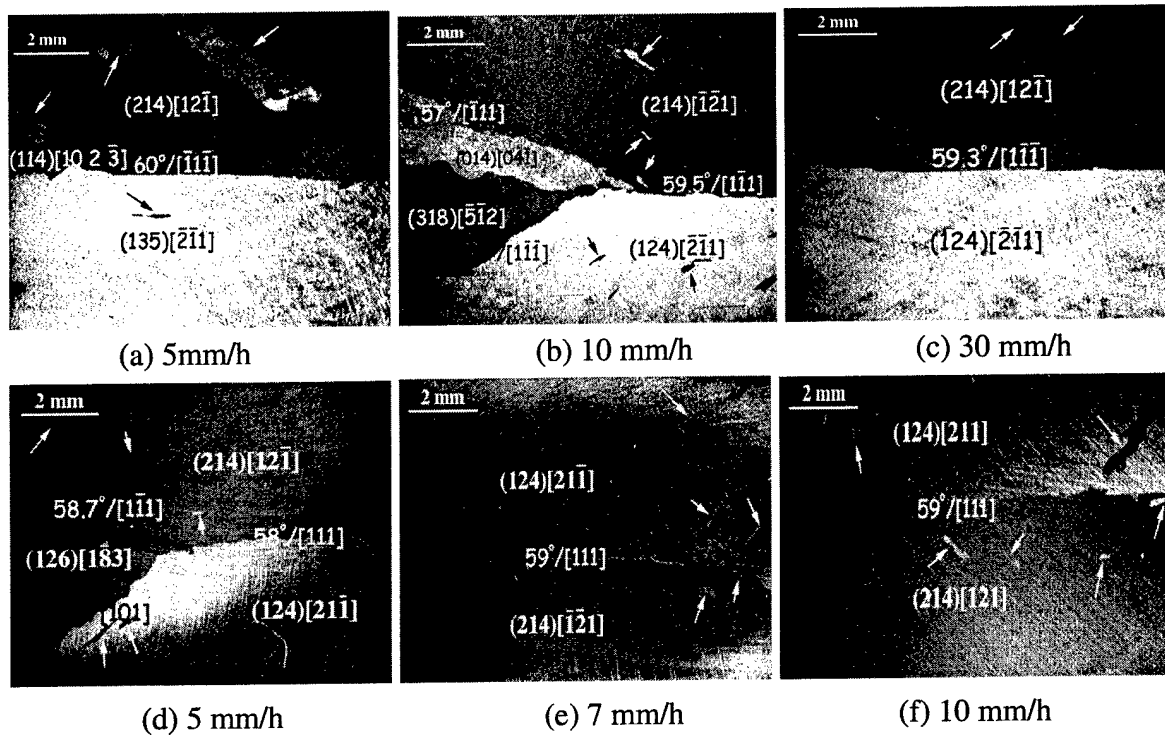


Figure 17. Directional annealing of (a,b,c) as-cold-rolled nickel and (d,e,f) cold-rolled nickel recrystallized for 30 min at 350° at 1000°C with a temperature gradient of 1000°C/cm at the hot zone speeds shown.

In order to investigate the origin of this directional recrystallization texture, cold-rolled nickel specimens were isothermally annealed for one hour at either 400, 500, 600, 700, 800, or 1000°C. It was found that a sharp cube texture was produced after 400°C annealing, and a  $\{124\}\langle 21\bar{1}\rangle$  texture appeared in the specimen annealed at 600°C, where abnormal grain growth or secondary recrystallization occurred. A sharp  $\{124\}\langle 21\bar{1}\rangle$  texture was also produced after 1000°C annealing. Therefore,  $\{124\}\langle 21\bar{1}\rangle$  is the preferred secondary recrystallization texture for cold-rolled nickel. Figure 18 shows one example of a large abnormally-grown grain from the specimen annealed at 600°C, in which the low angle ( $<15^\circ$ ), high angle random ( $>15^\circ$ ) and twin boundaries are in aqua, black and red, respectively. The large grain has an orientation of  $\{124\}\langle 21\bar{1}\rangle$ , and the small grains around it have a weak cube texture. The grain boundaries between the  $\{124\}\langle 21\bar{1}\rangle$  oriented large grains and the cube oriented small grains were often

near  $40^\circ/\langle 111 \rangle$ , which has been reported to have the maximum grain boundary mobility in unalloyed aluminum. Therefore, the formation of the  $\{124\}\langle 21\bar{1} \rangle$  orientation columnar grains and the secondary recrystallization texture are due to the anisotropic grain boundary mobility. Note that the small island grains left in the columnar grains were either twins or had low-angle boundaries.

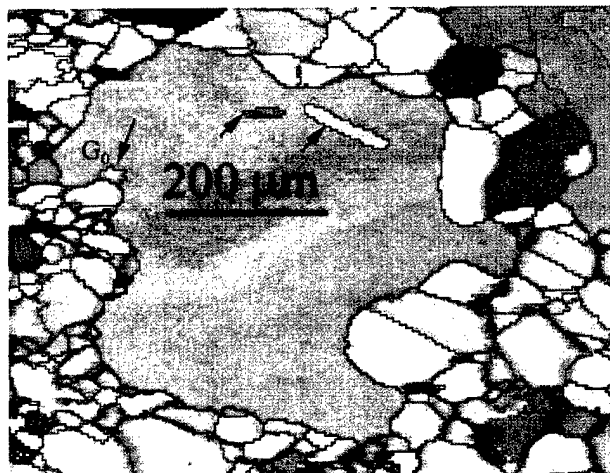


Figure 18. A  $\{124\}\langle 21\bar{1} \rangle$  grain in a specimen isothermally annealed for 1 hr at  $600^\circ\text{C}$ .

## Island grains in the directionally-recrystallized columnar grains

Small grains were often left behind the growth front, becoming island grains inside the columnar grains, see Figure 17. The orientations of several island grains were measured, and it was found that they had low angle misorientations or twin relationships with the columnar grains. In Figure 19(a) grains G1 and G4 are twins, and G2 has a low angle grain boundary.

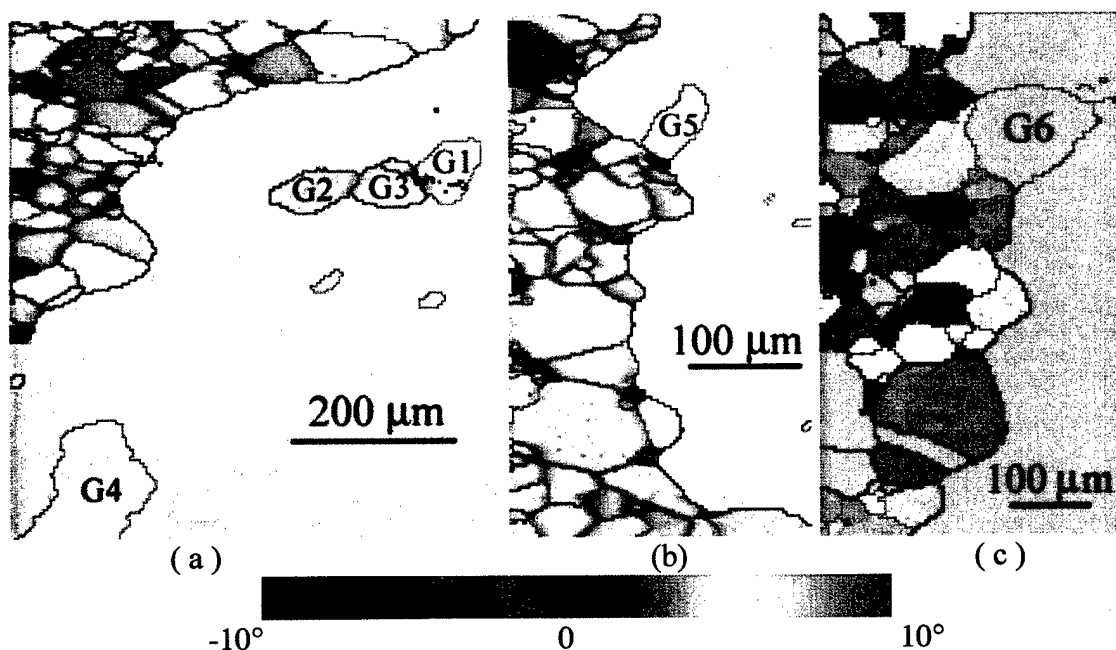


Figure 19. The growth front between columnar grains and small cube-oriented grains. The grain color indicates the misorientation offset from either the  $\{124\}\langle 21\bar{1} \rangle$  texture (a,b) or the cube texture (c). High angle boundaries are black, low angle boundaries are aqua and  $\Sigma 3$  twin boundaries are red.

G3 in Figure 19, which has a high angle boundary with the columnar grain, was probably left behind because it was between grains G1 and G2. The formation of a grain with a low angle boundary and a twin island grain is shown in Figure 19(b, c). The small grains in front of the hot zone are mostly cube oriented, and the boundaries between them are mostly low angle ( $<15^\circ$ ). Thus, the growth front mostly consists of high-angle, random boundaries for a  $\{124\}<21\bar{1}>$  oriented columnar grain. When the growth front passed over a grain which was either low angle or twin misoriented with respect to  $\{124\}<21\bar{1}>$ , a low angle or twin grain boundary will be formed in the growth front. This will act as a pinning point at the growth front. It is likely that G5 and G6 would have become island grains if the growth front had moved further. The formation of these low angle or twin island grains again indicates that the growth of the columnar grain structures is driven by the anisotropic grain boundary mobility.

### Personnel Supported

A. Y. Badmos	Post-Doctoral Fellow, Dartmouth College
J. Li	Graduate Student, Dartmouth College
H. J. Frost	Associate Professor of Engineering, Dartmouth College
I. Baker	Professor of Engineering, Dartmouth College

### Awards

Ian Baker was elected a Fellow of ASM International in 2001 and a Fellow of the Institute of Mining, Minerals and Materials in 2002.

### Publications

"Simulation of Microstructural Evolution During Directional Annealing", A.Y. Badmos, I. Baker, H.J. Frost, Recrystallization and Grain Growth, Eds., G. Gottstein and D.A. Molodov, Springer-Verlag, Germany, 2001, vol. 2, 1041-1046.

"Microstructural Evolution During Directional Annealing", A.Y. Badmos, H.J. Frost and I. Baker, *Acta Materialia*, **50** (2002) 3347-3359.

"The Effect of Hot Zone Velocity and Temperature Gradient on the Directional Recrystallization of Polycrystalline Nickel", J. Li, S.L. Johns B. Iliescu, H.J. Frost and I. Baker, *Acta Materialia*, **50** (2002) 4491-4497.

"Characterization of directionally recrystallized cold-rolled nickel using EBSP", B. Iliescu, J. Li and I. Baker, Proc. of Microscopy and Microanalysis 2002, 1264-5CD.

"Simulation of Microstructural Evolution During Directional Annealing with Variable Boundary Energy and Mobility", A.Y. Badmos, H.J. Frost and I. Baker, *Acta Materialia*, **51** (2003), 2755-2764.



**Presentations**

- "Directional Recrystallization Processing", A. Badmos, I. Baker and H.J. Frost, Fall TMS meeting, St Louis, Mo, 8-12 October, 2000.
- "Simulation of Microstructural Evolution during Directional Annealing", A. Badmos, I. Baker and H.J. Frost to be presented at the First Joint International Conference on Recrystallization and Grain Growth, Aachen, Germany, 27-31 August, 2001.
- "Simulation of Grain Growth during Directional Annealing", A. Badmos, I. Baker and H.J. Frost, poster to be presented at the Fall TMS meeting, Indianapolis, IN, 5-8 Nov., 2001.
- "Simulation of Directional Annealing", I. Baker, J. Li, A. Badmos and H.J. Frost, 2002 Annual TMS meeting, Seattle, WA, February 17<sup>th</sup> -21<sup>st</sup>, 2002.
- "Electron Back-Scatter Diffraction Pattern Study of Directionally Recrystallized MA 754 and Cold-Rolled Nickel", B. Iliescu, J. Li and I. Baker, poster at the 2002 Annual TMS meeting, Seattle, WA, February 17<sup>th</sup> -21<sup>st</sup>, 2002.
- "Directional Recrystallization of Cold-Worked Nickel", I. Baker, J. Li, B. Iliescu, B. Bollinger, A. Badmos and H.J. Frost, 2002 Fall TMS meeting, Columbus, OH, October 6<sup>th</sup>-10<sup>h</sup>, 2002.
- "Processing of Cold-Rolled Nickel by Directional Recrystallization" I. Baker, J. Li, B. Iliescu, A. Badmos and H.J. Frost, Ann. TMS meeting, San Diego, 2<sup>nd</sup>-6<sup>th</sup> March, 2003.